Attack Resilient Wireless Backhaul Connectivity with Optimized Fronthaul Coverage in UAV Networks

Xingqi Wu and Junaid Farooq
Department of Electrical and Computer Engineering,
University of Michigan-Dearborn, Dearborn, MI 48128 USA,
Emails: {xingqiwu, mjfarooq}@umich.edu.

2023 IEEE Conference on Communications and Network Security (CNS) | 979-8-3503-3945-1/23/$31.00 ©2023 IEEE | DOI: 10.1109/CNS59707.2023.10288893

***Abstract*—Multi-unmanned aerial vehicle (UAV) networks emerge as a viable solution, offering wireless coverage for dispersed Internet of Things (IoT) devices in remote and disaster struck areas. However, the placement of the UAVs plays a crucial role in the performance and resilience of the network. The UAVs need to cover all the ground users whilst staying in close proximity to sustain cyber attacks and failures, which is a non-trivial optimization problem since the users may have arbitrary locations. In this paper, we tackle the challenge of UAV placement optimization by cost-effectively providing both coverage and connectivity for end-to-end communication of spatially dispersed ground users or IoT devices. Our proposed approach leverages a two-step optimization framework that splits the UAVs according to their role of providing coverage or connectivity. Sequential execution of the optimization is able to generate the placement solutions that concurrently satisfy the requirements of user coverage and connectivity with fixed amount of UAVs. Simulation results show that the proposed framework can achieve resilient UAV formations compared to related works in the literature and is adaptive and scalable to a variety of user locations.**

***Index Terms*—unmanned aerial vehicles, connectivity, distributed algorithm.**

I. Introduction

Unmanned Aerial Vehicles (UAVs) are poised to play an increasingly critical role in addressing the challenges of providing comprehensive and efficient wireless communications to remote and rural regions [1]. Next-generation wireless cellular networks, such as 5G, have largely been focused on expanding wireless broadband connectivity. However, implementing wireless infrastructure in less populated and more geographically challenging areas has been met with reluctance by telecommunication providers. The reason lies in the fact that these deployments are less profitable compared to urban 5G infrastructure, causing a considerable gap in rural connectivity.

The Internet of things (IoT) has revolutionized various sectors such as environmental monitoring [2], surveillance [3], agriculture monitoring systems [4], healthcare [5], etc. However, these applications are largely dependent on reliable wireless connectivity. The absence of wireless infrastructure particularly hinders the proliferation of IoT-based applications in rural sectors. To bridge this gap, UAVs are being leveraged to create aerial communication networks. Serving as aerial base stations (BS), these UAVs can deliver wireless services to ground users and IoT devices through *fronthaul* links (shown by the blue dotted lines in Fig. 1) [6]. Concurrently, they also need to maintain *backhaul* links (shown by the bold dashed green lines in Fig. 1) with other aerial BSs, providing multi-hop wireless backhauling for seamless end-to-end connectivity among ground users [7]. Often, these UAVs have to operate in regions that are remote and may not have access to terrestrial connectivity.

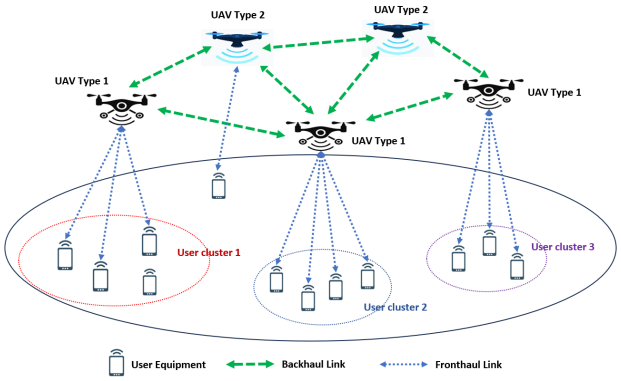

Fig. 1: Multi-UAV network providing coverage and backhaul connectivity to users on the ground in spatially dipersed clusters.

Ensuring comprehensive and consistent connectivity, especially in remote or disaster-stricken regions, where traditional network infrastructure may be lacking is a major concern. Ground users in these areas, including IoT devices, require reliable wireless coverage. UAVs have shown potential in these circumstances but optimizing their deployment for maximum coverage and connectivity, while being resilient to failures and attacks, is complex. By collaborating to form a multi-UAV network, UAVs can provide end-to-end wireless communication services to ground users, including IoT devices, within a specified operational area. However, the deployment and operation of such networks present a myriad of challenges in terms of their strategic placement for user coverage, number optimization, and backhaul connectivity, i.e., maintaining a connection among all UAVs in the network.

Traditional cellular networks employ direct wired or optical fiber-based backhauling, connecting base stations to the core network. This setup contrasts starkly with aerial communication networks, which rely on multi-hop UAV-based wireless backhauling [7]. Hence, to enable end-to-end communication between ground users, it is crucial to maintain both *coverage*, i.e., fronthaul links between ground users and UAVs, as well

as *connectivity*, i.e., backhaul links between UAVs to achieve end-to-end communication for users on the ground [8]. While coverage is user-centric, the connectivity needs to adopt a global view considering where the groups of users are located and how to orchestrate UAVs for connecting the dis-aggregate and dispersed groups of users. Additionally, the connectivity needs to be robust and resilient to achieve reliable end-to-end communication in case of UAV failure or cyber-physical attacks.

Several works in the literature tackle the problem of optimizing the placement in multi-UAV networks. These employ various objectives, such as ground-user coverage maximization [9]–[11], optimizing the number of UAVs needed [12], [13], ensuring backhaul connectivity [14]–[17], energy efficiency [18]–[20], and trajectory optimization [21]–[23], etc. However, most works do not consider the fact that these networks are prone to failures and adversarial attacks [24]. Hence, resilience must be a key consideration in the placement alongside performance optimization since a single failure may be enough to sabotage end-to-end communication.

In this paper, we focus on the optimized and resilient placement of UAVs, by maintaining the right balance between fronthaul and backhaul connectivity in multi-UAV networks. We approach the challenge by first casting the joint optimization problem into a two-step sequential optimization problem. This splitting allows us to approach the objectives of maximizing the user coverage and the resilient connectivity of UAVs independently. We then propose an iterative algorithm to find the optimal placement configuration of the UAVs.

The rest of this paper is structured as follows: Section II presents the system model, which outlines the formulation for establishing connectivity between UAVs and ensuring user coverage. In section Section III, we propose a two-step optimization approach to optimize the UAV placement. Section IV first introduces the metrics employed to evaluate the performance of our proposed approach and presents the results of the simulation experiments. Finally, section V concludes the paper.

II. System Model

In this section, we provide an overview of the system model, communication architecture used, and the UAV operating environment considered in the paper. Consider a set of M ground users denoted by U, where each user $u \in U$ is located in 2D space denoted as $l_u \in \mathbb{R}^2$. Let $l_u = \{x_u, y_u\}$ denote the Cartesian coordinates of the users, $l_u \in L_U$, where $L_U = \{l_1, l_2, l_3, ..., L_M\}$. Consider a set of N UAVs denoted by V with Cartesian coordinates $l_v = \{x_v, y_v, h\} \in \mathbb{R}^3$, where h denotes the height[1] of the UAVs. Each UAV is assumed to have a fronthaul communication range of $R_f \in \mathbb{R}$ and a backhaul communication range[2] of $R_b \in \mathbb{R}$. An illustration of the system model is shown in Fig. 2. The Euclidean distance between a user u and UAV v is denoted by $d_{u,v}$ and the Euclidean distance between UAV v and UAV w is denoted by $D_{v,w}$. While the height of UAVs can have a significant impact on the coverage range and hence, optimizing the height is crucial for optimal placement, however, the height can easily be incorporated into the optimization by considering each UAV to have a different communication range.

[1]We have limited ourselves to a uniform height for all UAVs for better visualization and analysis of the results. The consideration of effect of height is left for future extensions of this work.

[2]Note that the communication range can be determined based on a threshold over the minimum achievable data rate for coverage.

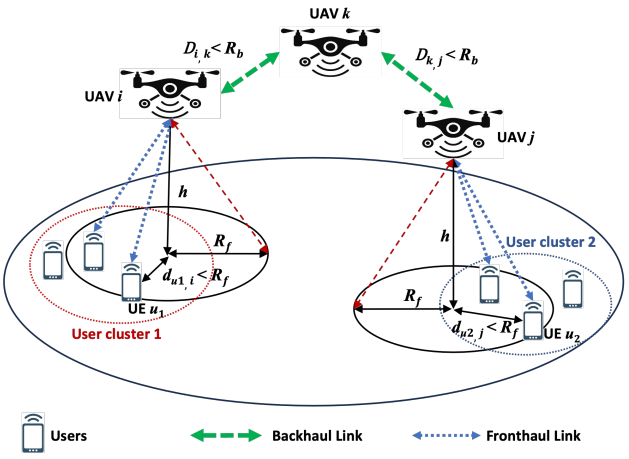

Fig. 2: System model. Here, UAV i and UAV j are providing coverage to ground users while UAV k is positioned to maintain connectivity between UAV i and j.

A. Problem Formulation

The key problem is to determine the best placement of UAVs that is able to maximize the coverage of ground users while ensuring that the UAVs stay connected to each other for backhaul communication. This can be formulated as follows:

$$\max_{\forall l_v \in \mathbb{R}^2} \sum_{u \in U} \mathbb{1}\left(\min_{v \in V} d_{u,v} \leq R_f\right), \tag{1}$$

$$d_{v,v'} \geq R_0 \quad \forall v, v' \in V, v \neq v', \tag{2}$$

$$\sum_{v' \in V, v' \neq v} \mathbb{1}\left(D_{v,v'} \leq R_b\right) \geq 1, \forall v \in \mathcal{J}, \forall \mathcal{J} \subset V, \tag{3}$$

where $\mathbb{1}(.)$ is the indicator function that returns 1 if the condition inside the parentheses is true, and 0 otherwise and $\mathcal{J}$ is the subset of UAV set V. R_0 is the minimum separation between UAVs. The objective in (1) is to ensure the maximum number of users are within the fronthaul communication range of at least one UAV, based on the Euclidean distance between the user and the closest UAV. While aiming for this objective, the model mandates that every UAV maintains a connection with at least one other UAV by being within a specified backhaul communication range R_b as reflected in (3), and simultaneously, all UAVs must respect a minimum separation distance R_0, as reflected in (2), to prevent interference or potential collisions.

Determining the optimal UAV locations presents a combinatorial optimization problem, with dual objectives of maximizing user coverage and guaranteeing UAV network connectivity. The

inherent challenge emanates from the NP-Hard nature of both the coverage objective and the connectivity constraint. This means that direct, exact solutions for the original optimization problem are elusive. While there exist various heuristic methods designed to find acceptable solutions, these objective heuristic approaches often falter when scaling up with the growing number of UAVs and diverse user typologies. They also carry the overhead of frequent hyper-parameter tuning. In light of these limitations, a two-step optimization process is proposed as a more robust and scalable solution to tackle this intricate problem.

III. Two-Step UAV Placement Optimization

To manage this complex optimization problem, we split up the UAVs into two distinct sets, each designed with a specific purpose in mind. Firstly, let V_1 represent the set of UAVs tasked with providing coverage, referred to as *Type 1* UAVs. The cardinality of this set is N_1, and each UAV $v \in V_1$ is positioned in a 3D space with Cartesian coordinates $l_{v_1} \in \mathbb{R}^3$. These coordinates can be expressed as $l_{v_1} = \{x_{v_1}, y_{v_1}, h\}$ where $l_{v_1} \in L_{V_1}$ and $L_{V_1} = \{l_{v_1}, l_{v_2}, ..., L_{v_{N_1}}\}$. Similarly, the set V_2 embodies the UAVs focused on ensuring connectivity, termed as *Type 2* UAVs. This set has cardinality N_2, where $N_1 + N_2 = N$ and each UAV $v_2 \in V_2$ is placed in a 3D space described by Cartesian coordinates $l_{v_2} \in \mathbb{R}^3$. These coordinates are denoted as $l_{v_2} = \{x_{v_2}, y_{v_2}, h\}$, with $l_w \in L_{V_2}$ and $L_{V_2} = \{l_{w_1}, l_{w_2}, ..., L_{w_{N_2}}\}$.

The placement is optimized for coverage and connectivity in a two-step process. The first step is focused on ensuring maximum coverage of users in spatially dispersed clusters. Hence, the first step optimization problem can be written as follows:

$$\min_{l_v} \mathcal{L}_1 = \left[\sum_{v \in V_1} \sum_{u \in U} f(d_{u,v}) + \alpha_1 \sum_{v,v' \in V_1, v \neq v'} \frac{1}{D_{v,v'} + \epsilon} \right], \tag{4}$$

where $f(.) : \mathbb{R} \rightarrow \mathbb{R}$ is a continuously differentiable, monotonously increasing function, α_1 is the penalty constant for close proximity of UAVs, and ϵ is a small constant, which ensures there is no division by zero. For the purposes of this paper, the function used is $f(x) = \sqrt{x}$, which corresponds to a square law path-loss[3]. The constant α_1 acts as a penalty for UAVs that are too closely located during the first step. The second step ushers in a new set of UAVs, V_2, intended to deliver backhaul connectivity across all UAVs. The objective function for this phase is:

$$\min_{l_w \in \mathbb{R}^2} \mathcal{L}_2 = \left[\sum_{w \in V_2} \sum_{v \in V_1} D_{w,v} + \alpha_2 \sum_{w,w' \in V_2, w \neq w'} \frac{1}{D_{w,w'} + \epsilon} + \alpha_3 \sum_{w \in V_2, v \in V_1} \frac{1}{D_{w,v} + \epsilon} \right]. \tag{5}$$

[3]Note that the function $f(.)$ can be selected based on the path-loss model used and will not change the optimization problem and solution methodology.

Here, α_2 and α_3 represent penalty constants addressing the proximity of UAVs within the second step and between both steps, respectively. The values of α_1, α_2, and α_3 can be adjusted based on user distribution and the upper bounds of the communication range.

A. Proposed Algorithm and Analysis

Given the smooth nature of our cost function, gradient-based methodologies are apt for optimizing the solution. We now describe the pseudocode for our proposed two-step optimization gradient algorithm, presented in Algorithm 1.

Algorithm 1 Placement Optimization Algorithm for Step χ

Input: Objective function $\mathcal{L}_\chi, \chi \in \{1, 2\}$ (either from Equation (4) or (5)), Number of UAVs: N_χ, Initial user locations, and Optimal Type 1 UAV locations (only for step 2), hyperparameters $\alpha_1, \alpha_2, \alpha_3$.

Output: Optimized locations of UAVs , i.e., $l_v^* \in V_1, \forall v$ and $l_w^* \in V_2, \forall w$ for step 1 and step 2 respectively.

1: Initialize UAV candidate locations uniformly in 2D space $L^0_{V_\chi}$.
2: Initialize optimization parameters: $\epsilon \leftarrow 10^{-6}$, $i_{\max} \leftarrow 10^4$.
3: Denote optimization vector $\mathbf{x} \leftarrow L_{V_\chi}, \chi \in \{1, 2\}$.
4: **for** i = 1 to $i_{\max}$ **do**
5: Compute Jacobian: $J \leftarrow \frac{\partial \mathcal{L}_\chi(\mathbf{x})}{\partial \mathbf{x}}$
6: Compute Hessian: $H \leftarrow \frac{\partial^2 \mathcal{L}_\chi(\mathbf{x})}{\partial \mathbf{x} \partial \mathbf{x}'}$
7: **if** $\|\mathcal{L}_\chi(\mathbf{x}) - \mathcal{L}_\chi(\mathbf{x} - H^{-1}J)\| < \epsilon$ **then**
8: **break**
9: **end if**
10: Update $\mathbf{x} \leftarrow \mathbf{x} - H^{-1}J$
11: **end for**
12: Output the result: $L^*_{V_\chi} \leftarrow \mathbf{x}$

return $L^*_{V_\chi}$

Initially, the algorithm sets random Type 1 UAV candidate locations based on a fixed number N_1, following a Gaussian distribution. For algorithmic control, two primary parameters, a convergence threshold ϵ and the maximum number of iterations $i_{\max}$, are determined. The heart of our approach employs Newton's Method to ascertain the optimal solution. Within each iteration, the algorithm computes the Jacobian (line 5) and the Hessian (line 6) matrices. Convergence is tracked (line 7) based on the change in the cost function. If the change is beneath threshold ϵ, the algorithm terminates. Otherwise, it updates the solution (line 10) and continues.

The algorithm is equally viable for the second step optimization. Post determining Type 1 UAV locations, the focus shifts to situating Type 2 UAVs. The algorithm starts by initializing Type 2 UAV locations, governed by N_2, using a Gaussian distribution. The process from line 1 to 11 resonate with the first step optimization, but calculations for the Jacobian and Hessian matrices pivot on (5). A noteworthy challenge in Algorithm 1 is the inversion of the Hessian matrix. Given the potential complications with the Hessian matrix, our primary version of the algorithm relies on its inversion. To address

these challenges and enhance efficiency, the Broyden-Fletcher-Goldfarb-Shanno (BFGS) [25] method can be used for updating H.

IV. Performance Evaluation

This section delves into the performance evaluation of the proposed algorithm through rigorous simulations. The ensuing subsections outline the performance metrics, provide an overview of the simulation settings, and present the resulting data.

A. Evaluation Metrics

To gauge the efficiency of our approach, we use two primary metrics, resonating with those employed in prior research:

1) **User Coverage Ratio:** Represents the percentage of users within the maximum fronthaul coverage range of all UAV types. This metric underlines the algorithm's ability to cover the maximum user populace.
2) **Strength of Connectivity between UAVs:** Using the Fiedler value—a second-smallest eigenvalue of the Laplacian[4] matrix denoted as $\lambda(L)$—we assess UAV connectivity. Calculated from the adjacency matrix A, a non-zero Fiedler indicates complete reachability among UAVs. A higher value signifies robust and dependable connectivity.

These metrics holistically evaluate our method's performance concerning user coverage and UAV connectivity.

B. Simulation Setup

In order to achieve a comprehensive understanding of the performance of our proposed framework, we conduct several simulations of multi-UAV network deployment in a two-dimensional plane, modeling a real-world operational environment where users are scattered on the ground plane. The user distribution follows a 2-D Gaussian mixture model, capturing actual user spatial distributions in varied environments. The operational area selected for UAV deployment spans 50 km by 50 km. The user clusters' centroids, represented by the mean of their distributions, are placed at $\mu_1 = [10, 10]^T$ and $\mu_2 = [50, 50]^T$. This positioning ensures that the users are not clustered at the center or at the extreme corners, but rather provide a more balanced distribution across the plane. With a variance matrix indicating no covariance, the user distribution within each cluster is symmetrical along both axes. This means that users are equally likely to be spread in all directions from the mean, maintaining a circular (rather than elliptical) dispersion. Moreover, the total user count stands at 200, evenly distributed among the two clusters, ensuring a balanced load and user representation from both clusters. Table I offers a breakdown of these parameters for clarity.

[4]Mathematically, the Laplacian matrix L is articulated as $L = \mathcal{D} - A$, where $\mathcal{D}$ is the degree matrix and A is the adjacent matrix.

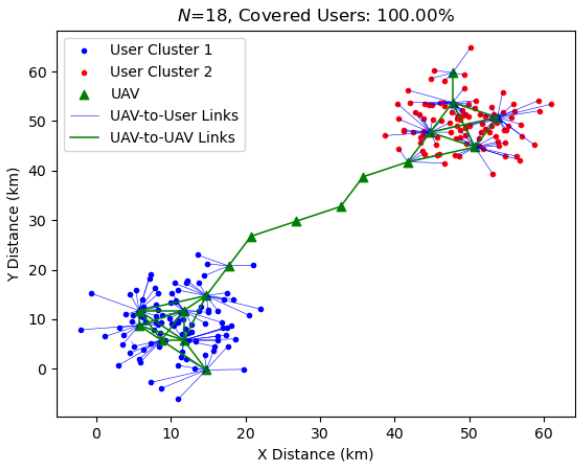

Fig. 3: UAV placement using the BaG Algorithm.

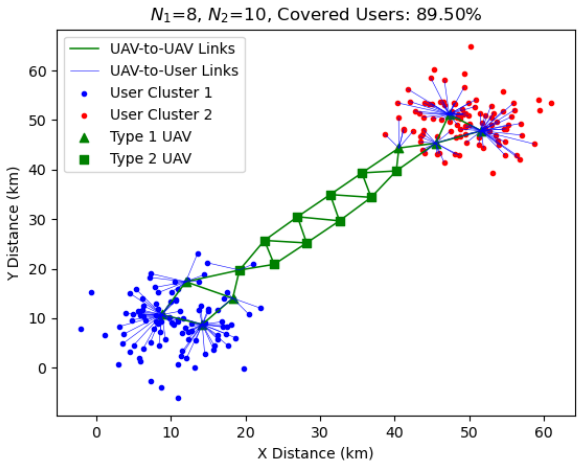

Fig. 4: Resilient UAV placement via the proposed method.

Parameters	Value
UAV deployment region	50 km × 50 km
Mean of user distribution	$\mu_1 = [10, 10]^T$, $\mu_2 = [50, 50]^T$
Variance of user distribution	$\Sigma_1 = \begin{bmatrix} 5 & 0 \\ 0 & 5 \end{bmatrix}, \Sigma_2 = \begin{bmatrix} 5 & 0 \\ 0 & 5 \end{bmatrix}$
Number of user clusters	2
Total number of ground users	200 (100 for each cluster)

TABLE I: Simulation Parameters.

C. Simulation Results and Discussion

As highlighted earlier, the deployment of Type 1 UAV is mainly optimized for user coverage, while it also strengthens the connectivity between UAVs as the number increases. The Type 2 UAVs are mainly deployed to enhance the UAV connectivity especially under situations where lesser Type 1 UAV are required to cover the most of the users.

Initially, we compare our proposed two-step optimization method against the established Backhaul-aware Greedy al-

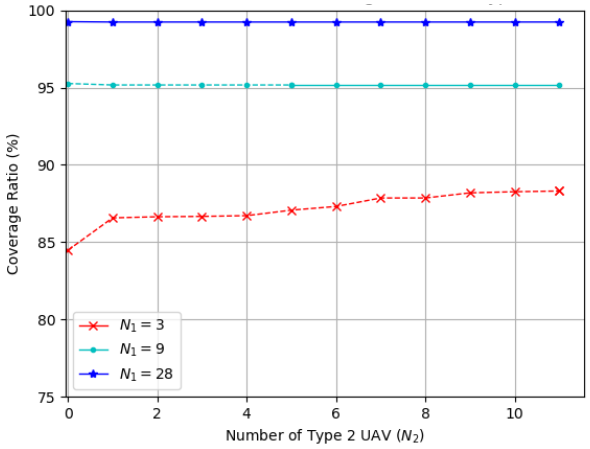

Fig. 5: Coverage ratio against the number of Type 2 UAVs.

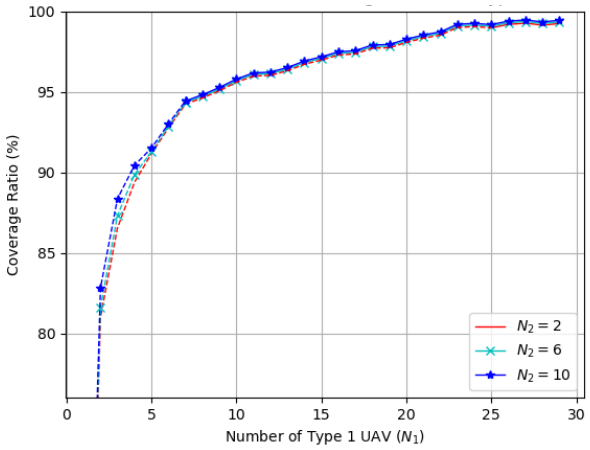

Fig. 6: Coverage ratio against the number of Type 1 UAVs.

gorithm (BaG) [12]. During these tests, ground users were dispersed in clusters as detailed in Table I. Both the maximum fronthaul and backhaul communication ranges, R_f and R_b, were set at 8 km. For equity, the BaG algorithm was first applied to determine the number of UAVs needed for total user coverage. Subsequently, our optimization was employed with this UAV count. Fig. 3 illustrates BaG's results, which unsurprisingly, used fewer UAVs for complete user coverage while maintaining inter-UAV connectivity. Conversely, Fig. 4 displays our method's results, which also confirmed backhaul UAV connectivity. Some UAVs even showcased multiple backhaul links, enhancing connectivity strength. However, our two-step method doesn't always assure full user coverage, but increasing Type 1 UAVs gradually nears a 100% coverage ratio with swift convergence.

Subsequent simulations assessed the interplay between coverage ratio and the counts of Type 1 and 2 UAVs, referencing Table I. To achieve representative results, each UAV combination was trialed 20 times, and average values were computed for both user coverage and connectivity. For these, R_f and R_b were both set at 10 km. Fig. 5 and Fig. 6 display

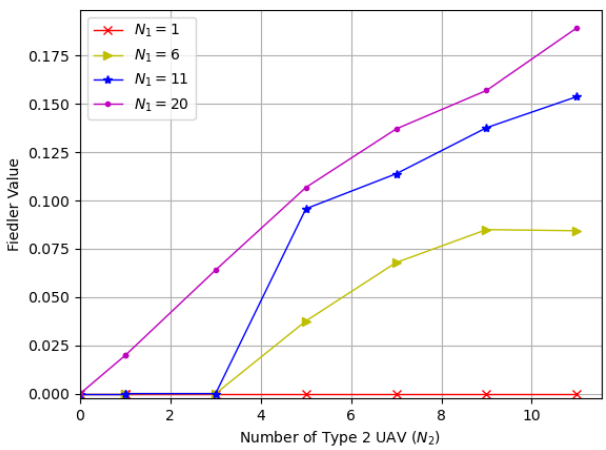

Fig. 7: Connectivity against the number of Type 2 UAVs.

the results. The former shows that user coverage remains largely unchanged with increasing Type 2 UAVs. However, introducing a sufficient number of Type 2 UAVs can markedly amplify connectivity, facilitating viable user coverage scenarios. Fig. 6 further underscores the dominance of Type 1 UAVs in determining user coverage.

A deeper exploration revealed the ties between UAV types and connectivity, especially gauged through the Fiedler value—a connectivity measure. Non-zero Fiedler values affirm complete UAV interconnectivity, with larger values indicating stronger connections. Fig. 7 maps the relationship between Type 2 UAV count and connectivity. Crucially, minimal Type 1 UAV counts lead to null Fiedler values, signaling a connectivity lapse. But increasing Type 1 UAVs reduces the need for Type 2 UAVs to maintain reachability. As anticipated, higher Type 2 UAV counts correspond with ascending Fiedler values, denoting stronger connectivity. Fig. 8, a heatmap, illustrates the relationship between the number of both Type 1 and Type 2 UAVs on connectivity. Some anomalies arise due to varied user cluster distributions and Type 2 UAV counts, especially when UAV numbers are limited. Yet, the overarching correlation between UAV counts and connectivity remains evident. Fig. 9 shows the performance of our proposed methods under attack varying random UAV failure probability with fixed number of Type 1 UAV. Consistent with results shown in Fig. 7, increasing number of Type 2 UAV deployment enhances the resilience of UAV connectivity.

V. Conclusion

In this paper, we address the challenge of formulating a placement strategy of multi-UAV network to ensure maximum wireless coverage to spatially dispersed ground users while maintaining resilient backhaul connectivity among the UAVs. We initially delineated the problem, and due to its NP-Hard nature, we transform the problem into a two-step optimization problem, where the sub-problems are focused on optimizing the objectives of coverage and connectivity separately. We then solved the problem using gradient based methods and

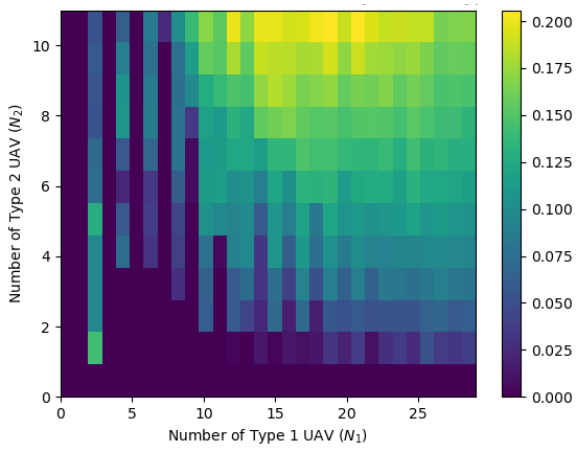

Fig. 8: Connectivity against the number of both Type 1 and Type 2 UAVs.

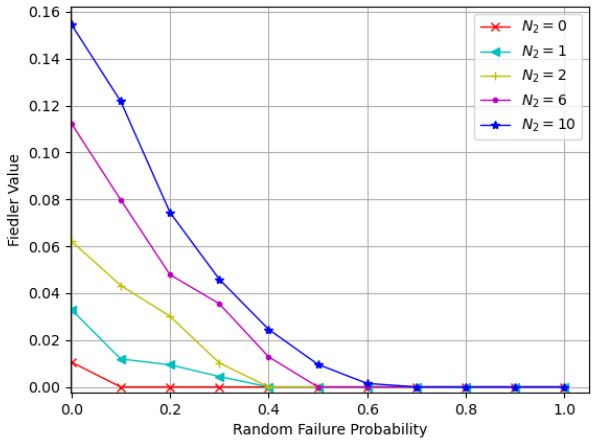

Fig. 9: Connectivity against random UAV failure, with $N_1 = 30$.

conducted extensive simulations to understand the interplay between the number of UAVs, user coverage, and network robustness and resilinece against failures and attacks. As we look ahead, our future endeavors will encompass the amalgamation of resilience-centric UAV placements with user association constraints, especially in scenarios dominated by highly mobile ground users.

REFERENCES

[1] E. Yaacoub and M.-S. Alouini, "A key 6G challenge and opportunity—connecting the base of the pyramid: A survey on rural connectivity," *Proceedings of the IEEE*, vol. 108, no. 4, pp. 533–582, 2020.

[2] M. Zhang and X. Li, "Drone-enabled Internet-of-things relay for environmental monitoring in remote areas without public networks," *IEEE Internet of Things Journal*, vol. 7, no. 8, pp. 7648–7662, 2020.

[3] W. Yu, Y. Liu, T. Dillon, W. Rahayu, and F. Mostafa, "An integrated framework for health state monitoring in a smart factory employing IoT and big data techniques," *IEEE Internet of Things Journal*, vol. 9, no. 3, pp. 2443–2454, 2022.

[4] A. Pagano, D. Croce, I. Tinnirello, and G. Vitale, "A survey on LoRa for smart agriculture: Current trends and future perspectives," *IEEE Internet of Things Journal*, vol. 10, no. 4, pp. 3664–3679, 2023.

[5] P. Verma and S. K. Sood, "Fog assisted-IoT enabled patient health monitoring in smart homes," *IEEE Internet of Things Journal*, vol. 5, no. 3, pp. 1789–1796, 2018.

[6] M. K. Shehzad, A. Ahmad, S. A. Hassan, and H. Jung, "Backhaul-aware intelligent positioning of uavs and association of terrestrial base stations for fronthaul connectivity," *IEEE Transactions on Network Science and Engineering*, vol. 8, no. 4, pp. 2742–2755, 2021.

[7] K. Wu, K.-W. Chin, and S. Soh, "UAVs deployment algorithms for maximizing backhaul flow," *IEEE Systems Journal*, pp. 1–12, 2023.

[8] Y. Wang and J. Farooq, "Resilient UAV formation for coverage and connectivity of spatially dispersed users," in *IEEE International Conference on Communications (ICC 2022)*, 2022, pp. 225–230.

[9] C. Zhang, L. Zhang, L. Zhu, T. Zhang, Z. Xiao, and X.-G. Xia, "3D deployment of multiple uav-mounted base stations for UAV communications," *IEEE Transactions on Communications*, vol. 69, no. 4, pp. 2473–2488, 2021.

[10] M. Nafees, J. Thompson, and M. Safari, "Multi-tier variable height UAV networks: User coverage and throughput optimization," *IEEE Access*, vol. 9, pp. 119 684–119 699, 2021.

[11] T. Kimura and M. Ogura, "Distributed collaborative 3D-deployment of UAV base stations for on-demand coverage," in *IEEE Conference on Computer Communications (INFOCOM 2020)*, 2020, pp. 1748–1757.

[12] J. Sabzehali, V. K. Shah, Q. Fan, B. Choudhury, L. Liu, and J. H. Reed, "Optimizing number, placement, and backhaul connectivity of multi-UAV networks," *IEEE Internet of Things Journal*, vol. 9, no. 21, pp. 21 548–21 560, 2022.

[13] B. Cao, M. Li, X. Liu, J. Zhao, W. Cao, and Z. Lv, "Many-objective deployment optimization for a drone-assisted camera network," *IEEE Transactions on Network Science and Engineering*, vol. 8, no. 4, pp. 2756–2764, 2021.

[14] Y. Zhou, Z. Gu, J. Zhang, and Y. Ji, "Efficient deployment of aerial relays in FSO-based backhaul networks," *Journal of Optical Communications and Networking*, vol. 15, no. 1, pp. 29–42, 2023.

[15] Z. Rahimi, R. Ghanbari, A. H. Mohajerzadeh, H. Ahmadi, and M. Sookhak, "3D UAV BS positioning and backhaul management in cellular network via stochastic optimization," in *IEEE Global Communications Conference (GLOBECOM 2022)*, 2022, pp. 2169–2175.

[16] S. A. Al-Ahmed, M. Z. Shakir, and S. A. R. Zaidi, "Optimal 3D UAV base station placement by considering autonomous coverage hole detection, wireless backhaul and user demand," *Journal of Communications and Networks*, vol. 22, no. 6, pp. 467–475, 2020.

[17] N. Iradukunda, Q.-V. Pham, M. Zeng, H.-C. Kim, and W.-J. Hwang, "UAV-enabled wireless backhaul networks using non-orthogonal multiple access," *IEEE Access*, vol. 9, pp. 36 689–36 698, 2021.

[18] B. Omoniwa, B. Galkin, and I. Dusparic, "Optimizing energy efficiency in UAV-assisted networks using deep reinforcement learning," *IEEE Wireless Communications Letters*, vol. 11, no. 8, pp. 1590–1594, 2022.

[19] H. Zhang, J. Zhang, and K. Long, "Energy efficiency optimization for NOMA UAV network with imperfect CSI," *IEEE Journal on Selected Areas in Communications*, vol. 38, no. 12, pp. 2798–2809, 2020.

[20] D. Zhai, C. Wang, R. Zhang, H. Cao, and F. R. Yu, "Energy-saving deployment optimization and resource management for UAV-assisted wireless sensor networks with NOMA," *IEEE Transactions on Vehicular Technology*, vol. 71, no. 6, pp. 6609–6623, 2022.

[21] Z. Xu, D. Deng, Y. Dong, and K. Shimada, "Dpmpc-planner: A real-time uav trajectory planning framework for complex static environments with dynamic obstacles," in *2022 International Conference on Robotics and Automation (ICRA)*, 2022, pp. 250–256.

[22] X. Wu, Z. Wei, Z. Cheng, and X. Zhang, "Joint optimization of UAV trajectory and user scheduling based on NOMA technology," in *2020 IEEE Wireless Communications and Networking Conference (WCNC)*, 2020, pp. 1–6.

[23] L. Dong, Z. Liu, F. Jiang, and K. Wang, "Joint optimization of deployment and trajectory in UAV and IRS-assisted IoT data collection system," *IEEE Internet of Things Journal*, vol. 9, no. 21, pp. 21 583–21 593, 2022.

[24] A. Raja, L. Njilla, and J. Yuan, "Adversarial attacks and defenses toward AI-assisted UAV infrastructure inspection," *IEEE Internet of Things Journal*, vol. 9, no. 23, pp. 23 379–23 389, 2022.

[25] J. D. Head and M. C. Zerner, "A broyden—fletcher—goldfarb—shanno optimization procedure for molecular geometries," *Chemical Physics Letters*, vol. 122, no. 3, pp. 264–270, 1985. [Online]. Available: https://www.sciencedirect.com/science/article/pii/0009261485805741